Materials Chemistry and Physics 253 (2020) 123126

Contents lists available at ScienceDirect

Materials Chemistry and Physics

journal homepage: www.elsevier.com/locate/matchemphys

Formation of Moiré superstructure of epitaxial graphene on Pt(111): A molecular dynamic simulation investigation

Bin Sun [a,*], Wenze Ouyang [b,**], Jianbing Gu [a], ChenJu Wang [a], Jianjun Wang [c], Liwei Mi [a]

[a] School of Materials and Chemical Engineering, Zhongyuan University of Technology, Zhengzhou, 450007, PR China
[b] Key Laboratory of Microgravity, National Microgravity Laboratory, Institute of Mechanics, Chinese Academy of Sciences, Beijing, 100190, PR China
[c] Center for Quantum Functional Materials and Design, College of Science, Zhongyuan University of Technology, Zhengzhou, Henan, 450007, China

HIGHLIGHTS

- Used CMD method to study the moiré structures of the graphene on Pt(111) surface.
- Observed some structures with the same properties as that of Merino's model.
- Investigated the graphene fluctuation, C–C bond length and the stress of C atoms.
- Discussed the formation mechanism of the structure with ultra-long periodicity.

ABSTRACT

The moiré superstructures formed in the graphene on Pt (111) surface have been studied employing classical molecular dynamics (CMD) simulation. We have shown that the 20 moiré superstructures, whose positions and periodicities are the same as the prediction of the geometric model proposed by Merino, can be obtained via the rotation of graphene. This observation demonstrates that molecular dynamics simulation is an effective method for searching for moiré superstructure formed in the graphene on transition metal surface. The characteristics of moiré superstructures, such as fluctuation of the graphene layer, C–C bond length and stress of carbon atoms, are investigated. For the superstructures with large periodicity, the graphene layer is fluctuant. In the region of the maximal height of the superstructure, there is a strong attraction between the graphene and Pt substrate, so that the carbon atoms are concave, and the C–C bonds are stretched by 0.0004 Å. In the region of the minimal height of the superstructure, the C–C bond lengths are the same as those in freestanding graphene. Additionally, a moiré superstructure with an ultra-long periodicity (L = 60.1 Å) is observed, and its formation mechanism is discussed.

1. Introduction

Chemical vapor deposition (CVD) on transition metal (TM) surfaces represents a promising approach to achieve reasonably uniform high-quality monolayer graphene. For this purpose, the growth of graphene is carried out on the surfaces of a series of TM substrates [1–4]. Scanning tunneling microscope (STM) images have proved the existence of moiré superstructures in the graphene/TM system due to the spatial coincidence of the atomic periodicity of the graphene lattice with that of the supporting metal [5,6]. Formation of moiré superstructures has been reported on many metals, such as Ru [7,8], Ir [9,10], Rh [11], Pt [12,13], and recently Cu [14], Pd [15], Co [16], and Ni [17]. In these systems, the moiré superstructure acts as a smooth superpotential that varies slowly compared to the one associated with carbon atoms. The corresponding unit cell, which is larger than the one of pristine graphene, is associated with replica Dirac cones, reduced Fermi velocity [18,19], with either superlattice Dirac cones [20，21] or mini-gaps [21] at the moiré Brillouin zone boundary. Such properties make this system an ideal playground to investigate quantum phases arising in periodic two-dimensional electron gases subjected to an external magnetic field [20–22].

Pt(111) substrate is of distinctive interest because the Pt substrate has the minimum effect on the physical properties of graphene due to very weak graphene-substrate interaction dominated by van der Waals (vdW) forces [23]. The moiré superstructures of the graphene on Pt(111) show more complicated periodicities and orientations. The first STM investigation was reported by Land et al., in 1992 [24], in which the small graphite island (about 20–30 Å in diameter), namely moiré superstructure in nature, was observed. Works published later showed evidence of the existence of more moiré superstructures [25]. Gao et al.

* Corresponding author.
** Corresponding author.
E-mail addresses: sunbin7610@sina.com (B. Sun), oywz@imech.ac.cn (W. Ouyang).

https://doi.org/10.1016/j.matchemphys.2020.123126
Received 16 September 2019; Received in revised form 28 March 2020; Accepted 25 April 2020
Available online 11 June 2020
0254-0584/

[13] had grown the monolayer graphene on Pt(111) surface by chemical decomposition of ethylene. The hexagonal moiré superstructures containing 2 × 2, 3 × 3, 4 × 4, ($\sqrt{37} \times \sqrt{37}$)R21, ($\sqrt{61} \times \sqrt{61}$)R26, ($\sqrt{67} \times \sqrt{67}$)R12 were observed, and the proportions of different moiré superstructure depended on the substrate temperature. Sutter et al. [12] used *in situ* low-energy electron microscopy to investigate the growth and structure properties of graphene on Pt(111). Their studies had shown that the lattice mismatch between graphene and Pt(111) was accommodated by moiré structure with a large number of different rotational variation. Fast and slow growing graphene domains exhibited moiré structures with small [e.g., (3 × 3), ($\sqrt{6} \times \sqrt{6}$)R2, and(2 × 2)R4] and large unit cells [e.g.,($\sqrt{44} \times \sqrt{44}$)R15, ($\sqrt{52} \times \sqrt{52}$)R14, (8 × 8)], respectively.

The first principle calculation is also an ideal means for investigating the interfacial interaction and the properties of the moiré superstructure. Wang et al. [26] used DFT to study the 12C/11Rh moiré superstructure of graphene on Rh(111), and Gao et al. [13] employed DFT to investigate the geometric structure and electronic structure of graphene on Pt(111). These results showed good agreement with experiments and explained many interesting properties from the atomic-scale viewpoint, such as the fluctuation of the graphene layer and the change of bond length. However, for such weakly bound system as graphene/Ir(111) or graphene/Pt(111), the most commonly used exchange-correlation functionals [local density approximation(LDA) and generalized gradient approximation (GGA)] lack the nonlocal-correlation effects responsible for van der Waals (vdW) interaction, which results in an imprecise height of the carbon adsorbate and very low binding energies of per C atom. The nonlocal-correlation functional vdW DF was developed and successfully applied to simple vdW-bonded systems. Busse et al. [27] applied the nonlocal van der Waals density functional approach to calculate the binding of graphene to Ir(111). They found the bonding of graphene to Ir(111) to be due to the van der Waals interaction with an antibonding average contribution from chemical interaction. In certain areas of the large graphene moiré unit cell charge accumulation between Ir substrate and graphene C atoms is observed, signaling a weak covalent bond formation.

Although there is a large number of works devoted to the studies of the moiré structures, there are not many systematic studies determining all the emerging experimental superstructures appearing in graphene/TM systems. Merino proposed a geometrical model to investigate the origin of the coincidence moiré superstructure in 2011 [28]. This model predicted the formation of 22 stable superstructures for graphene on Pt (111). Another geometrical model had been proposed by K. Hermann [29], which predicted moiré patterns of graphene on hexagonally-packed metal surfaces through their spatial beating frequencies. These geometrical models are successful in predicting possible moiré structures. However, it is important to point out that these models only take into account very simple geometrical considerations and overlook the effects of interfacial interactions [25,30]. Such interfacial interaction between graphene and metal substrate can bring about lattice deformation of graphene, thereby forming the more complex and elusive moiré superstructures.

Classical molecular dynamics (CMD) simulation can deal with larger simulation systems than the first-principles approach (such as density functional theory, DFT). However, for the TM substrates with strong interaction with graphene, such as Ru, Ni et al., the results of CMD simulation have been reported in few cases due to the lack of reliable interaction potential. Pt(111) surface has a weak interaction with graphene, allowing graphene with random orientations to grow on the Pt surface [12]. Extensive researches suggest that for such graphene-substrate systems with weak physisorption as graphene/Cu (111) [31,32] and graphene/Pt(111) [33–35], the dominant interaction between the graphene and substrate is the van der Waals (vdW) force which can be very accurately covered by simple interaction potentials, such as LJ potentials. In this paper, we attempt to use CMD simulation as an alternative method to search for possible moiré superstructures in the graphene/Pt(111) system. The 21 superstructures are found by rotating the graphene on the surface of Pt(111). Additionally, fluctuation of the graphene layer, C–C bond length and stress of carbon atoms in the graphene are analyzed and discussed.

2. Details of molecular dynamics simulation

To reproduce the experimentally found moiré structures, classic molecular dynamic (CMD) simulations are performed. The model for CMD simulation is built as displayed by Fig. 1(a) and (b). A three-layer slab model of Pt (111) surface containing 19834 atoms is built. Above the surface of Pt, monolayer graphene with a width of 9.4 nm and length of 13.4 nm is placed. The initial separation distance between the Pt(111) surface and the graphene layer is set as 3.0 Å. Periodic boundary condition (PBC) is adopted in all directions.

CMD simulation is carried out as the following procedures. Firstly the energy of the whole system is minimized by the conjugate gradient (CG) algorithm, and then the system is relaxed at the temperature of 30 K for 10ps time. Next, we perform a rotation operation of graphene around the fixed axis, ranging from 0° to 30° with the rotation speed of 0.18°/ps. The rotation angle, a relative angle between Pt(111) surface and the graphene, is called as Φ. In the case of formation of a moiré superstructure when the graphene rotates to a particular angle Φ, the letters Ω and L are used to denote the apparent angle and periodicity of moiré superstructure. Here, the apparent angle Ω represents the angle between the lattice vectors of moiré structure and the Pt[11(_)0] direction. Because of the symmetry of the system, the angular range of rotation angle Φ (0°–30°) can cover all the possible moiré superstructure [28]. Notice that the imposed rotation of graphene will bring out great stress in the system. To eliminate the stress, a relaxation with 5ps time is carried out every rotation angle of 0.36°. All the CMD simulations are performed in the canonical ensemble (NVT ensemble) with a time step of 0.5 fs and a Nosé–Hoover thermostat. The Ovito software has been utilized for displaying atomic and nanoscale structures [36].

The embedded atom potential is used to describe Pt–Pt interactions, which has been proven to be capable of describing the structural and mechanical properties of Pt [37]. The Tersoff potential proposed by Thompson in 1990 [38] is used to describe the interaction among carbon atoms, which gives a C–C bond length of 0.142 nm, and is identical to the experimental result [39]. For the cross-interactions at the interface, we employ a 12–6 Lennard-Jones (LJ) potential to describe Pt–C interactions [33–35]. The LJ parameters used here are$\sigma = 2.936$ Å and$\varepsilon =$ 0.04092eV, and the cutoff distance is set to 9.0 Å [40]. We have shown that with these parameters, the calculated equilibrium distance between the graphene layer and Pt(111) surface is 3.05 Å, which is very close to the value of 3.19 Å arising from DFT calculation [25]. The corresponding average adhesive energy of per carbon atom calculated by the LJ potential parameters is 38.89 meV, which is in good agreement with the results of first-principle calculation (38.6 meV–39.8 meV) [13]. It is noted that the interaction between the carbon atoms at the edge of the graphene layer and the Pt substrate below cannot be handled by the LJ pair potential due to the edge effect. In other studies, the researchers solved this problem by perfectly designing the size of the simulation cell and precisely matching the boundaries of graphene and Pt substrate. In our simulation work, the carbon atoms at the edge are treated in the same way as the carbon atoms in the middle. The reason for ignoring the edge effect is that the size of the graphene model built by us is large, and the edge effect has little impact on the mechanical properties of carbon atoms in the middle. Therefore, we can investigate the moiré superstructure by observing the features of the carbon atoms in the middle of the graphene layer.

In our previous studies, we had shown that the choice of three simulation parameters is vital to forming more moiré phases. The first is the appropriate simulation temperature. Previous studies have shown that too high temperature will wrinkle graphene and break its high

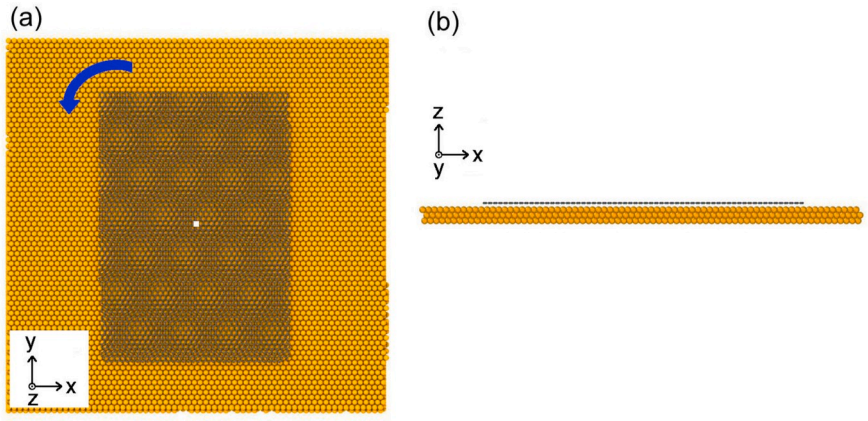

Fig. 1. Model used in CMD simulation. Monolayer graphene of 9.4 × 13.4 nm is placed above a square Pt slab. The separation distance between Pt(111) surface and graphene is 3.0 Å. The Pt slab is fixed and the graphene layer can rotate around a fixed axis (i.e. z-axis). The yellow and dark-grey spheres represent Pt and C atoms, respectively. The blue arrow indicates counterclockwise rotation of the graphene layer. The white dot located at the center of the graphene layer represents the section of the rotation axis. (a) Top view of the model; (b) Side view of the model. (For interpretation of the references to color in this figure legend, the reader is referred to the Web version of this article.)

symmetry [41]. Thus the simulation temperature should be set as low as possible, which is 30 K in our work. The second is to freeze all the Pt atoms rather than the Pt atoms on the bottom layer. The purpose of fixing all Pt atoms is to only deform the lattice of graphene. In this way, more orderly moiré patterns could be observed during the rotation process. It should be noted that although all the Pt atoms are fixed, the Pt–C interactions are still functional, which can modulate the deformation of graphene lattice to match Pt(111) lattice. An appropriate Tersoff potential is another key factor. The Tersoff potential proposed by Thompson in 1990 [38] is employed in our CMD simulation, which can result in the formation of experimental graphene with a lattice constant of 2.46 Å. For other kinds of Tersoff potentials (e.g., the references [42–44]), the lattice constant of graphene obtained is larger (2.53 Å) than that of experimental results.

CMD simulations have been carried out in the Large Scale Atomic/Molecular Massively Parallel Simulator (LAMMPS) package developed by Plimpton [45] at Sandia National Laboratories. Dell computer workstation with 8 cores, 16 threads, and CPU model i7-7700 is used to perform CMD calculation. For the present simulation model with 24520 atoms, the calculation speed is very fast, reaching almost 25

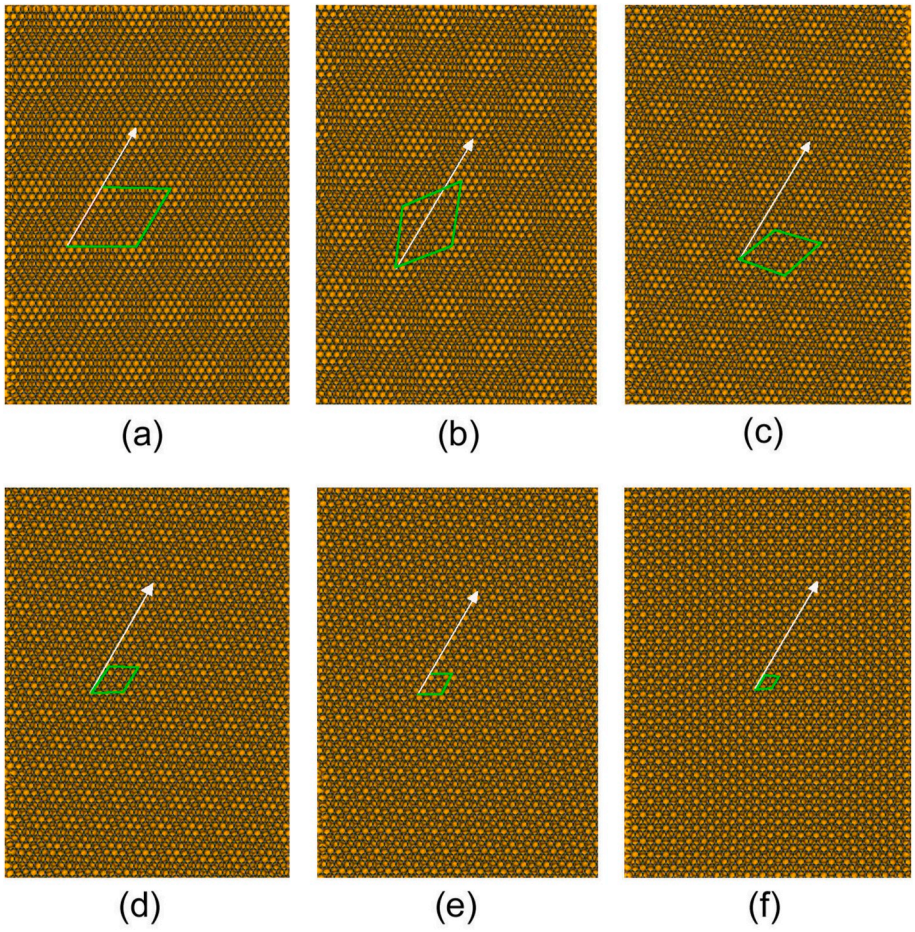

Fig. 2. Atomic snapshots of six rotational graphenes on Pt(111) surface . From (a) to (f), the rotation angles $\Phi = 0°$, 2.7°, 7.2°, 13.9°, 19.1°, and 30°, respectively. The Pt[11(_)0] direction is indicated by the white arrows and moiré unit cells are depicted as light green rhombuses. (For interpretation of the references to color in this figure legend, the reader is referred to the Web version of this article.)

steps/second.

3. Results and discussion

After the minimization of energy and relaxation of the whole system, the graphene begins to rotate counterclockwise on the Pt(111) surface around the rotation axis. Interestingly a series of moiré superstructures with different periodicities can form at different rotation angles Φ. In Fig. 2, six of them are presented as examples. From Fig. 2 (a) to (f), Φ = 0°, 2.7°, 7.2°, 13.9°, 19.1°, and 30°, respectively. When Φ = 0° [see Fig. 2(a)], the periodicity of the formed superstructure is L = 22.1 Å, which means 9 × 9 graphene lattice exactly matches 8 × 8 Pt(111) lattice. The lattice vector of the moiré structure is aligned with the Pt [11(_)0] direction, i.e. Ω = 0. When Φ = 2.7°, the moiré structure with L = 19.5 Å and Ω = 20.5 begins to form, as shown in Fig. 2(b). When Φ increases to 19.1°, a 3 × 3 superstructure with L = 7.4 Å forms, as shown in Fig. 2(e). When Φ = 30°, the formed moiré superstructure has a periodicity L = 4.9 Å and the apparent angle Ω = 0 [see Fig. 2(f)], which is a 2 × 2 superstructure often observed during the epitaxial growth of graphene [13].

In the range of Φ = 0°–30°, a serial of moiré phases have been searched and 20 superstructures are found, as listed in Table 1. We compare our results with those of the geometrical model proposed by Merino [28] (see left part of Table 1), finding that our 20 moiré superstructures are in agreement with those of the geometrical model except two superstructures (The numbers are 5 and 17, respectively). This consistency is reflected in two aspects. One is the position of moiré structure formation (i.e. the value of Φ), and the other is the periodicity of moiré structure (i.e. the value of L). Although the results obtained by two different methods, i.e., the CMD simulation and the geometrical model, are almost identical, there are some slight differences. For instance, the Ω values of 10 superstructures are the same or almost the same, but it is not the case for another 10 superstructures. Besides, another interesting phenomenon is that when the rotation angle is 30°, a superstructure with an ultra-long periodicity (L = 60.1 Å) comes into being (defined as the number 23 in Table 1), which has not been observed in experiments or other models yet.

Table 1
The rotation angles Φ, the periodicity L and apparent angle Ω of formed moiré superstructures in our CMD simulation (the right part of the table). To compare with the reference, the results of the reference are listed on the left of the table. The symbol × in the table represents not finding this superstructure.

	Reference			Our Results			
	Φ (deg)	L(Å)	Ω(deg)	Φ (deg)	L(Å)	Ω(deg)	
1	0	22.1	0	0	22.1	0	9 × 9
2	0.8	21	6.6	0.8	21	6.6	$\sqrt{73} \times \sqrt{73}$
3	1.3	22.5	12.2	1.3	22.5	11.8	$\sqrt{84} \times \sqrt{84}$
4	1.7	20.1	13.9	1.7	20.1	13.0	$\sqrt{67} \times \sqrt{67}$
5	2.1	21.9	19.1	×	×	×	
6	2.7	19.5	21.8	2.7	19.5	20.5	$\sqrt{63} \times \sqrt{63}$
7	3.7	19.2	30	3.7	19.2	30	$\sqrt{61} \times \sqrt{61}$
8	4.7	17	25.3	4.7	17	27	$\sqrt{48} \times \sqrt{48}$
9	5.7	17.2	16.1	5.7	17.2	21	$\sqrt{49} \times \sqrt{49}$
10	7.2	15.4	8.9	7.2	15.4	15.5	$\sqrt{39} \times \sqrt{39}$
11	9	13.7	0	9	13.7	9.5	$\sqrt{31} \times \sqrt{31}$
12	10.9	11.3	0	10.9	11.3	9.5	$\sqrt{21} \times \sqrt{21}$
13	12.4	21	6	12.4	21	6	$\sqrt{73} \times \sqrt{73}$
14	13.9	9.8	13.9	13.9	9.8	0	4 × 4
15	16.1	17.2	16.1	16.1	17.2	0	7 × 7
16	19.1	7.4	19.1	19.1	7.4	0	3 × 3
17	22.1	17.2	16.1	×	×	×	
18	23.1	22.5	12.2	23.1	22.5	12.0	$\sqrt{84} \times \sqrt{84}$
19	23.9	21.9	19.1	23.9	12.3	0	5 × 5
20	25.1	15.4	8.9	25.1	15.4	16	$\sqrt{39} \times \sqrt{39}$
21	26.1	20.1	13.9	26.1	20.1	13.1	$\sqrt{67} \times \sqrt{67}$
22	30	4.9	30	30	4.9	0	2 × 2
23				30	60.1	26	

Up to now, the total number of periodic graphene superstructures forming on Pt(111) is still unknown. DFT has shown its ability to study large unit cells for particular moiré superstructures, but it is an unattainable task to perform a full optimization of all possible superstructures (e.g., looking for the most favorable rotational angles and all possible coincidences between graphene and substrate unit cells) in DFT. The geometric model proposed by Merino is successful in searching for superstructures, but it has defects and limitations as it predicts the formation of superstructures only through geometric mismatch and does not take into account interaction between atoms. Although there are still some unexplained results in the present CMD simulation, the fact that the 20 moiré superstructures obtained in CMD simulation are consistent with the results of the geometric model proves the validity of the CMD method. Therefore, the CMD simulation used in this work would be a more intuitive and practical method for searching for the moiré superstructure formed in the graphene on transition metal surface.

As to the reasons why identical results can't be obtained by CMD simulation and geometric model (e.g., not observing 2 superstructures with numbers 5 and 17, different rotation angles Φ of 10 superstructures et al.), we will investigate further in our future studies. Here, we only state possible reasons. In the geometric model, the bond length between carbon atoms in graphene can't be changed. Therefore, the formation of the moiré superstructure is determined by lattice mismatch degree. In the present CMD simulation, as discussed in the following section, the bond lengths between carbon atoms can vary, and its variation scope is different in the different regions of graphene, which leads to the results that the moiré superstructures obtained by the geometric model do not necessarily appear in our CMD simulation. To simplify the simulation model in our work, the immobilized platinum atoms in the substrate are assumed, which is inconsistent with the real physical situation. Other CMD studies have shown that the metal lattice on the Pt substrate can also deform during the superstructure formation process [46]. Thus there are some subtle differences between our results and experimental observation.

The potential energy of each C atom is recorded in the simulation process. Fig. 3 shows the color-maps of the potential energy of C atoms in the graphene. The rotation angle Φ in Fig. 3 is the same as that in Fig. 2. Seen from Fig. 3, potential energy maps can exhibit moiré patterns more clearly than an atomic snapshot, indicating that the potential energy of C atom is variable in a different region of graphene. For superstructures with large periodicities, such as Fig. 3(a) and (b), C atoms located at the vertex of the superstructure have smaller potential energy, and the potential energy of C atoms around them increases gradually. Referring to the reference [7], we consider the area of the superstructure vertex as the region of maximal height and the area of the center of three vertexes as the region of minimal height. In the region of maximal height, the potential energy of the C atom is lowest, while the potential energy of surrounding C atoms increases gradually. In the region of minimal height, the potential energy reaches the largest value. This result indicates that the van der Waals (vdW) interaction between carbon atoms and the platinum substrate is stronger in the regions of maximal height, while it becomes weaker in the regions of minimal height. For the superstructures with smaller periodicities, the variation of potential energy also has this trend. Also, the moiré structure with the largest periodicity 60.1 Å can be presented more clearly through potential energy map, as shown in Fig. 3(f). In the later section, we will discuss the formation mechanisms for this structure.

The stability of different moiré phases is an important issue, i.e., which moiré superstructure is easiest to form? Here the adhesive energy between Pt substrate and graphene for different moiré structures is calculated based on the following formula [47].

$$E_{adhesive} = E_{total} - E_{Pt} - E_G$$

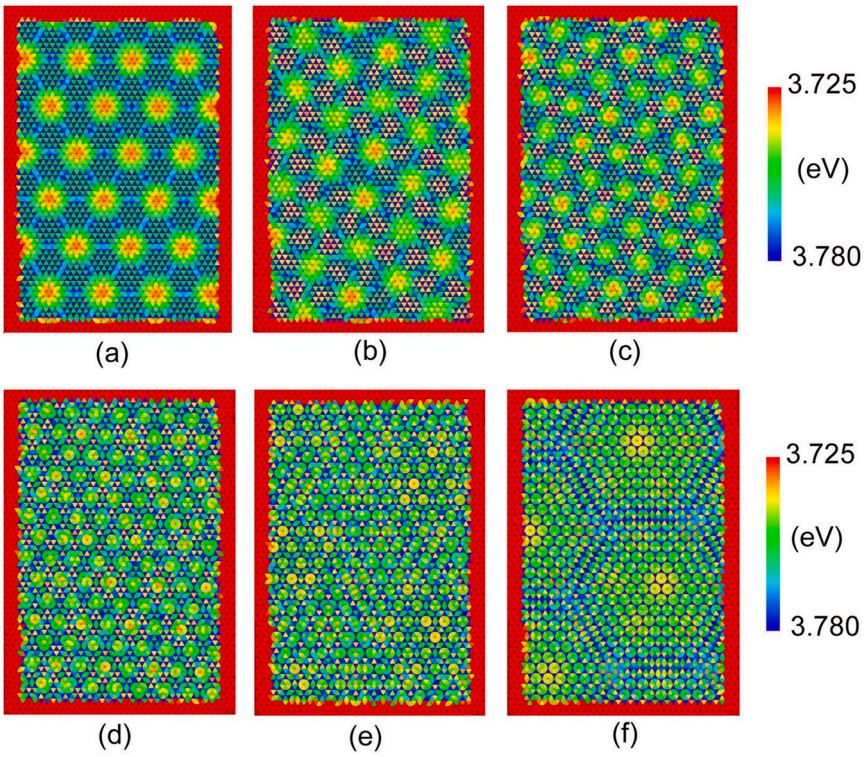

Fig. 3. Potential energy maps of carbon atoms in the graphene. From (a) to (f), the rotation angles Φ = 0°, 2.7°, 7.2°, 13.9°, 19.1°, and 30°, respectively.

Where E_{total} is the total potential energy of the whole system, E_{Pt} and E_G are the potential energy of Pt substrate and the graphene, respectively.

Fig. 4 shows the variation of average adhesive energy per carbon atom with the rotation angle Φ of the graphene. The black solid line represents the variation of average adhesive energies, and the red crosses represent the positions where the 20 moiré superstructures form. As can be seen from Fig. 4, the average adhesive energy per carbon atom changes in a small range (about 0.64 meV), indicating that the stability of the system changes very little at different rotation positions in terms of thermodynamics. The results could also explain an experimental phenomenon in which several kinds of moiré superstructures can coexist when the graphene grows on a platinum substrate. It can also be seen from Fig. 4 that the rotation positions where the moiré superstructure occurs are not necessarily the local maxima of the adhesive energy. Some of the rotation positions are more stable than the ones where the moiré superstructure forms. This result indicates that this kind of moiré superstructure is probably not observed in the experiments, which could be assumed as an unsteady moiré structure. The fundamental reason for the generation of moiré superstructure involves the geometrical factors of the mismatch between the graphene lattice and the platinum lattice, while the local maxima of the adhesive energy correspond to the position where the graphene sheet and the platinum substrate can form a better binding. Therefore, for such a moiré superstructure that does not occur at the local maxima of the adhesive energy, the corrugation and deformation of graphene is a good tradeoff to get better binding with the platinum substrate beneath it.

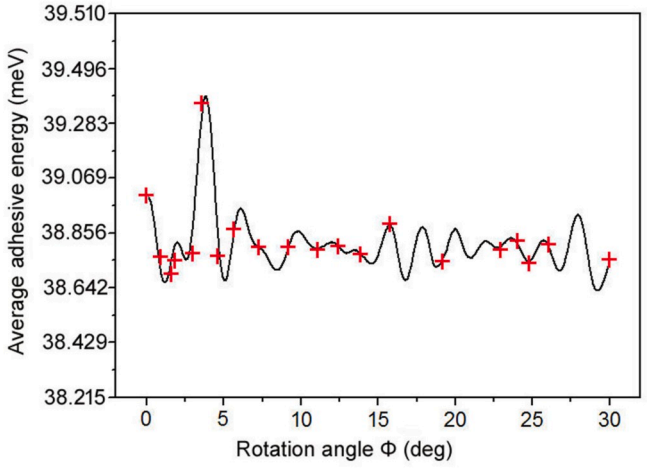

Fig. 4. Average adhesive energy between each carbon atom in the graphene and the Pt atoms below with the varying Φ in the CMD simulation. The black solid line represents average adhesive energy per carbon atom, and the red crosses show the rotation positions where the moiré superstructures formed. (For interpretation of the references to color in this figure legend, the reader is referred to the Web version of this article.)

Experimental observations and DFT studies have shown that graphene layer on the surface of the transition metal substrate is not flat, but corrugated [7,8,12–14,46]. For example, the superstructure formed in the graphene on Ru (0001) surface can form a hump with a height of about 1.67 Å [8]. The height variation of graphene on Pt (111) surface is also investigated in this work. Fig. 5 shows the color-maps of graphene heights for 3 moiré structures, where the periodicities are large [see Fig. 5 (a), L = 22.1 Å)], middle [see Fig. 5 (b), L = 9.8 Å] and small [see Fig. 5 (c), L = 4.9 Å], respectively. As the Pt surface is frozen, the height of carbon atoms in graphene, i.e. their z coordinates, can reflect the corrugation of the graphene layer. Obviously, for the superstructure with large periodicity, the graphene layer is uneven. The carbon atoms located in the regions of maximal height are concave, while those in the regions of minimal height are raised. The height difference between the highest and lowest position is about 0.4 Å. This value is slightly smaller than that observed in the experiment, where the height difference is 0.5 Å0.8 Å [13]. As the periodicity gets short, the fluctuation becomes little, and the height difference between the maximal height and the minimal one also decreases. For atypical superstructure with small periodicity L = 4.9 Å [Fig. 5(c)], the whole graphene layer seems flat and there is almost no fluctuation.

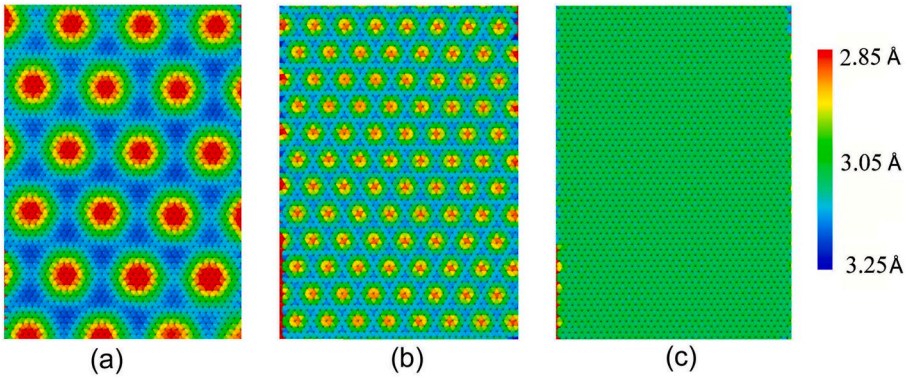

Fig. 5. Corrugation height of the graphene layer with respect to the Pt(111) surface. (a) Φ = 0 and L = 22.1 Å; (b) Φ = 13.9 and L = 9.8 Å; (c) Φ = 30 and L = 4.9 Å.

Another important modulation effect of Pt(111) surface on the graphene layer is a variation of bond lengths of carbon atoms. In order to induce the graphene lattices to match Pt(111) lattices, the C–C bonds in the graphene layer can be stretched or compressed [7,28]. By setting the different cutoff radius of bond length in Ovito software, we can precisely measure the changes of bond lengths in different regions of the graphene layer. As an example, Fig. 6 shows the variations of bond lengths for the moiré superstructures with the periodicity L = 22.1 Å. It can be seen from Fig. 6(a) that the bond length of the carbon atoms in the regions of minimal height and the radial direction around the regions of maximal height is about 1.4200 Å, which is the same as that of freestanding graphene. When the cutoff radius increases to 1.4204 Å [see Fig. 6(c)], the carbon atoms in the regions of maximal height are bonded, while the carbon atoms in the tangential direction around the regions of maximal height are not bonded to other atoms. These results indicate that the bond lengths of carbon atoms in the regions of maximal height are about 1.4204 Å, while the bond length in the tangential direction is larger than 1.4204 Å.

Here, we analyze the possible mechanisms of these phenomena by taking into account the results of Figs. 3, Figs. 5 and 6. In the regions of minimal height, the van der Waals (vdW) interaction between carbon atoms and the platinum substrate is weaker, which means that the graphene hardly interacts (there may be even a repulsion) with the Pt substrate, so the bond length is the same as that of freestanding graphene. In the regions of maximal height, the van der Waals (vdW) attractive interaction between carbon atoms and the platinum substrate becomes stronger, leading to the stretched C–C bonds, which also bring about the concave morphology of graphene layer.

The variation of bond lengths will inevitably lead to nonuniform stress distribution in the graphene layer. Fig. 7 shows the stress distribution maps of three typical moiré superstructures (Φ = 0°, 13.9°, and 30°, respectively). The maps of stress distribution in the z-direction are identical to the moiré patterns shown in Fig. 3. In the present model, the stress of carbon atoms in the z-direction mainly comes from the

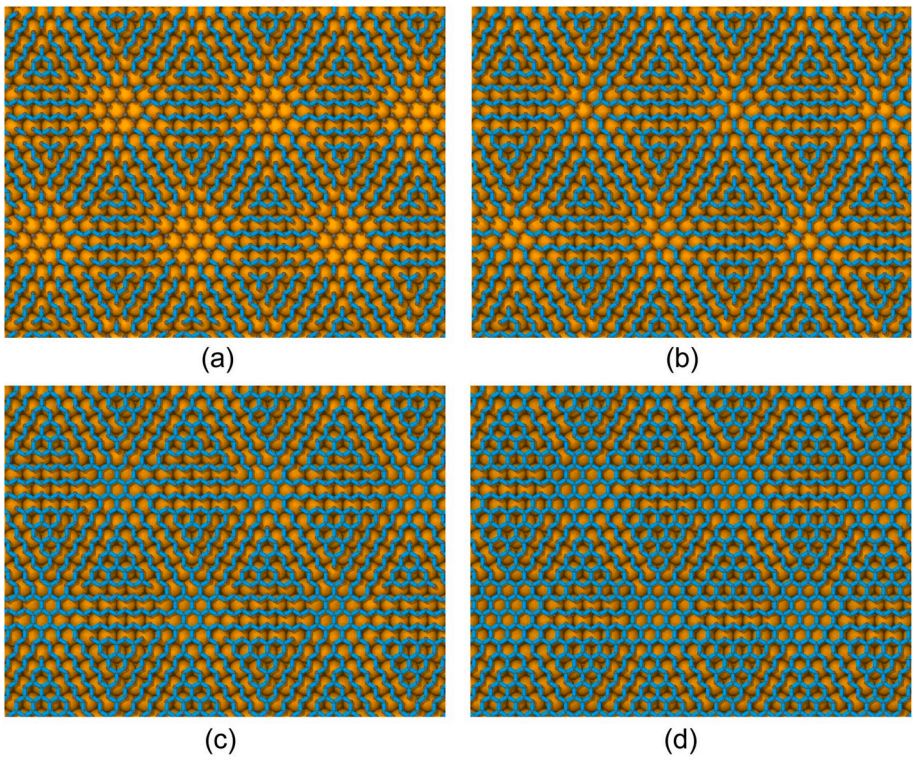

Fig. 6. Creation of C–C bonds in the graphene at a different cutoff radius of bond length. The cutoff radii of bond length are (a) 1.4200 Å, (b) 1.4202 Å, (c) 1.4204 Å, (d) 1.4206 Å, respectively. The periodicity L = 22.1 Å. The yellow and dark-grey spheres represent Pt and C atoms, respectively, and the sky-blue short bars represent C–C bonds. (For interpretation of the references to color in this figure legend, the reader is referred to the Web version of this article.)

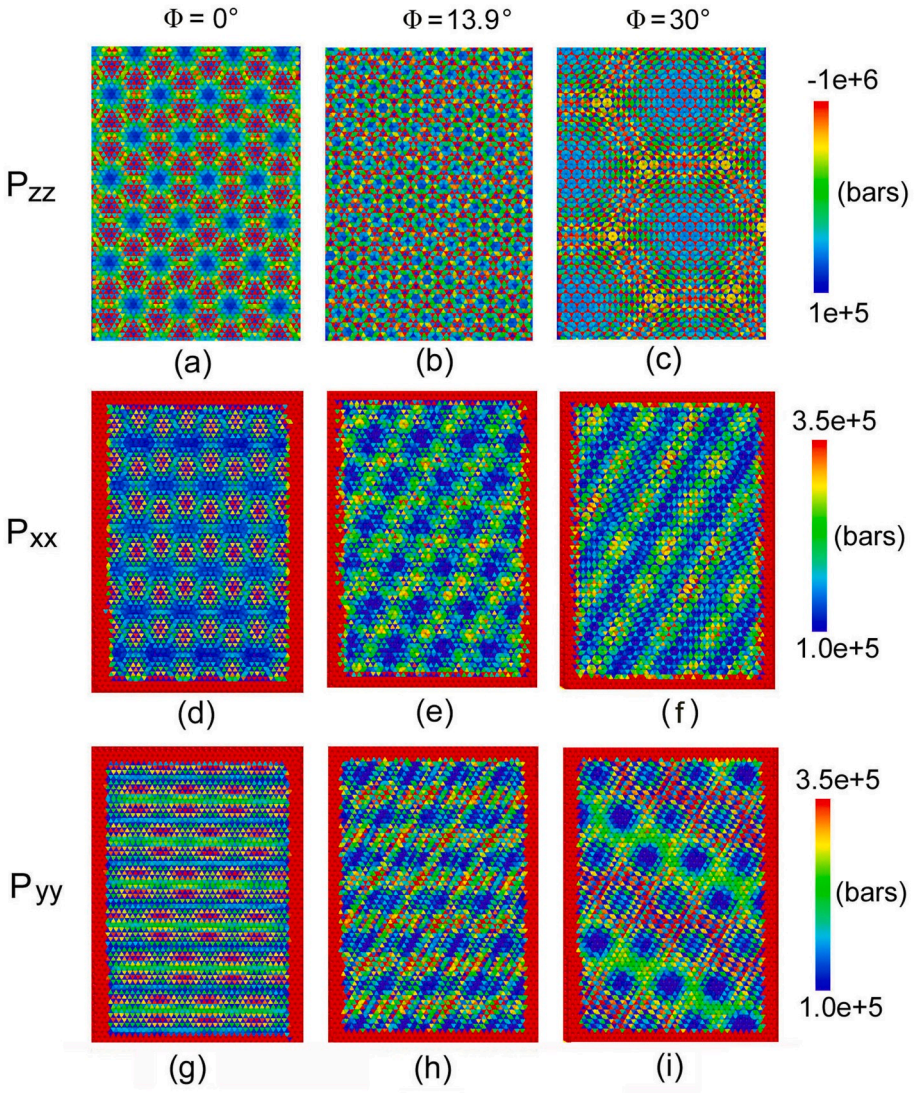

Fig. 7. Stress distribution maps of three typical moiré superstructures. The rotation angles Φ for three typical moiré superstructures are 0°, 13.9°, and 30°, respectively. The upper [(a), (b) and (c)], middle [(d), (e) and (f)] and bottom panels[(g), (h) and (i)] are the maps of stress distribution in z, x and y direction, respectively.

interaction between graphene and Pt substrate. Therefore, this observation indicates that the interaction between graphene and Pt substrate is also periodic. In the region of the maximal height of the superstructure, z stress is positive, indicating the carbon atoms of graphene and Pt substrate have a strong attraction. This result is consistent with the observations of Figs. 3 and 5, where the carbon atoms located in the regions of maximal height forms a concave morphology due to attraction interaction. Horizontal stress (in the x-direction and y-direction) is mainly caused by the variation of C–C bond length. Seen from the middle and bottom panels of Fig. 7, the horizontal stress distribution is too complex to know its regularity clearly. However, we can confirm that the stress of all carbon atoms in the horizontal direction is positive.

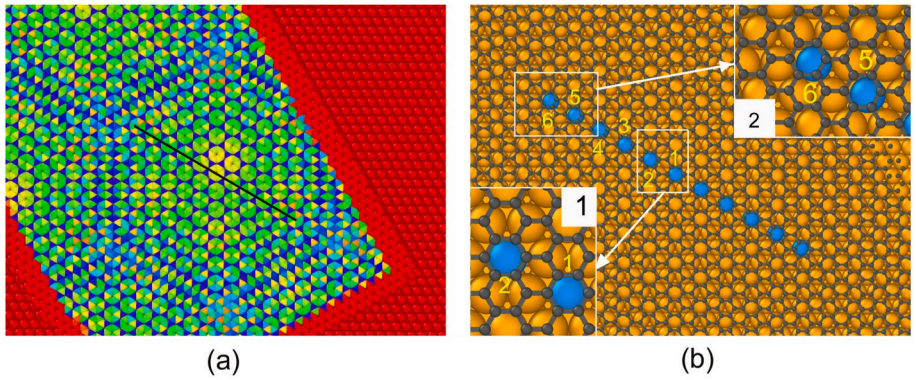

Fig. 8. Formation mechanism of the superstructure with ultra-long periodicity (L = 60.1 Å). (a) Potential energy maps. The 11 2 × 2 superstructures in the middle row are marked by black solid lines; (b) Atomic snapshot of the superstructure with ultra-long periodicity. The 11 Pt atoms corresponding to 11 2 × 2 superstructures are labeled in blue color. The insets 1 and 2 are enlarged images of two regions, respectively. Light yellow numbers 1–6 are used to label Pt atoms corresponding to 2 × 2 superstructures. (For interpretation of the references to color in this figure legend, the reader is referred to the Web version of this article.)

This implies that the whole graphene layer is under the tensile stress state, and the magnitude of stress would be dependent on the different regions.

Another novel observation needed to be discussed is the formation mechanism of the superstructure with ultra-long periodicity [Fig. 3(f)]. Fig. 8 displays the formation mechanism of this superstructure. This ultra-long periodic structure has a regular hexagonal shape, consisting of 102 2 × 2 small-period moiré superstructures. Let us concentrate on the middle row of 2 × 2 superstructures, which are marked by black solid lines. The potential energy map is converted into an atomic snapshot shown in Fig. 8 (b), where the Pt atoms corresponding to these 11 2 × 2 superstructures are labeled in blue color. Obviously, when the graphene rotates 30°, the zigzag direction of graphene is exactly aligned with the Pt[11(_)0] direction, and the formed 2 × 2 superstructures are certainly located in this direction. When 2 × 2 superstructures form, the Pt atom labeled 1, which is in the middle of 11 Pt atoms, is just located in the middle of the graphene ring, matching the lattice of graphene well [see the inset 1 of Fig. 8 (b)]. In the Pt[11(_)0] direction, the lattice periodicity of Pt substrate is 4.8047 Å, i.e., the distance between two Pt atoms in blue color is 4.8047 Å. Meanwhile, the lattice period of graphene is 2.46 Å, and the distance between two 2 × 2 superstructures is 4.9200 Å. Thus it leads to a distance difference of 0.1153 Å. This distance difference accumulates gradually from the center to the edge of the ultra-long superstructure, making the blue Pt atom labeled 6 not match the graphene lattice well (the mismatch has reached 23%), as shown in the inset 2 of Fig. 8 (b). Therefore, once the distance exceeds the sixth blue Pt atom, the 2 × 2 superstructure cannot form due to a large mismatch, and a non-periodic structure similar to grain boundary appears on the boundary of the ultra-long periodic structure.

Based on a detailed investigation above, it is easy to find that the moiré superstructure formed in Fig. 8 (b) is the same as the reconstruction model proposed by Otero et al. [48], which is called a second-order coincidence superlattice of the $(\sqrt{3} \times \sqrt{3})$ R30. In this model, one surface Pt atom is missing per$(\sqrt{3} \times \sqrt{3})$ R30 unit cell, and the rest of the Pt atoms are alternatively in the top or hollow positions with respect to the graphene layer. This reconstruction model is an energetically stable structure as it releases the stress of elastic distortions in the graphene layer due to a large mismatch between Pt and graphene meshes.

4. Conclusions

In this paper, the moiré superstructures of graphene formed on Pt (111) surface has been studied by classical molecular dynamics (CMD) simulation. 20 superstructures with different angles and periodicities are obtained via the rotation of graphene. The positions and periodicities of these 20 superstructures are exactly the same as those obtained by the geometric model proposed by Merino. This fact reveals that molecular dynamics simulation is an effective method for searching for moiré superstructures of the graphene formed on the transition metal surface. Compared with the geometric model and DFT, CMD simulation not only considers the interaction between atoms but also can deal with the model system with tens of thousands of atoms, which makes it possible to find some superstructures with ultra-long periodicity.

The properties of moiré superstructures obtained by CMD simulation are analyzed. For the superstructures with large periodicities, such as L = 22.1 Å, the graphene layer is uneven. The carbon atoms located in the regions of maximal height is concave, while the carbon atoms located in regions of minimal height is raised. The height difference between the highest and lowest positions is about 0.4 Å. For the superstructure with small periodicity L = 4.9 Å, the whole graphene layer appears flat. The variation of bond lengths of carbon atoms is also investigated. In the regions of minimal height, the bond lengths are the same as those of freestanding graphene (1.4200 Å). While in the regions of maximal height, the bonds are stretched by 0.0004 Å, which is caused by the interactions between the carbon atoms and the Pt atoms below. The conclusions of the above two properties are consistent with those of the stress distribution. In the regions of the maximal height of the superstructure, there is a strong attraction between the carbon atoms of graphene and Pt substrate, so the whole graphene is under the tensile stress state, and the magnitude of stress would be dependent on the different regions.

Declaration of competing interest

We declare that we have no financial and personal relationships with other people or organizations that can inappropriately influence our work, there is no professional or other personal interest of any nature or kind in any product, service and/or company that could be construed as influencing the position presented in, or the review of, the manuscript entitled.

CRediT authorship contribution statement

Bin Sun: Conceptualization, Funding acquisition. **Wenze Ouyang:** Supervision. **Jianbing Gu:** Investigation. **ChenJu Wang:** Validation. **Jianjun Wang:** Writing - original draft. **Liwei Mi:** Writing - review & editing.

References

[1] Z. Xu, T. Yan, G. Liu, G. Qiao, F. Ding, Large scale atomistic simulation of single-layer graphene growth on Ni(111) surface: molecular dynamics simulation based on a new generation of carbon-metal potential, Nanoscale 8 (2016) 921–929.
[2] T. Wu, X. Zhang, Q. Yuan, J. Xue, et al., Fast growth of inch-sized single-crystalline graphene from a controlled single nucleus on Cu–Ni alloys, Nat. Mater. 15 (2016) 43–47.
[3] B.Y. Dai, L. Fu, Z.Y. Zou, M. Wang, H.T. Xu, S. Wang, et al., Rational design of a binary metal alloy for chemical vapor deposition growth of uniform single-layer graphene, Nat. Commun. 2 (2011) 522–527.
[4] Z.Y. Zou, L. Fu, X.J. Song, Y.F. Zhang, Z.F. Liu, Carbide-forming groups IVB-VIB metals: a new territory in the periodic table for CVD growth of graphene, Nano Lett. 14 (2014) 3832–3839.
[5] L.Y. Zhu, F. Ding, How the moiré superstructure determines the formation of highly stable graphene quantum dots on Ru(0001) surface, Nanoscale Horizons (2019).
[6] Z. Zou, V. Carnevali, M. Jugovac, et al., Graphene on nickel (100) micrograms: modulating the interface interaction by extended moiré superstructures, Carbon 130 (2018) 441–447.
[7] W. Moritz, B. Wang, M.L. Bocquet, et al., Structure determination of the coincidence phase of graphene on Ru(0001), Phys. Rev. Lett. 104 (2010) 136102.
[8] D. Jiang, M.H. Du, S. Dai, First-principles study of the graphene/Ru(0001) interface, J. Chem. Phys. 130 (2009) 74705.
[9] J. Coraux, A.T. N'Diaye, T. Michely, C. Busse, Structural coherency of graphene on Ir(111), Nano Lett. 8 (2008) 565–570.
[10] E. Loginova, S. Nie, K. Thürmer, N.C. Bartelt, K.F. McCarty, Defects of graphene on Ir(111): rotational domains and ridges, Phys. Rev. B 80 (2009), 085430.
[11] H.G. Zhang, H. Hu, Y. Pan, et al., Graphene-based quantum dots, J. Phys. Condens. Matter 22 (2010) 302001.
[12] P. Sutter, J.T. Sadowski, E. Sutter, Graphene on Pt(111): growth and substrate interaction, Phys. Rev. B 80 (2009) 245411.
[13] M. Gao, Y. Pan, L. Huang, et al., Epitaxial growth and structural property of graphene on Pt(111), Appl. Phys. Lett. 98 (2011), 033101.
[14] L. Gao, J.R. Guest, N.P. Guisinger, Epitaxial graphene on Cu(111), Nano Lett. 10 (2010) 3512–3516.
[15] Y. Murata, E. Starodub, B.B. Kappes, C.V. Ciobanu, et al., Orientation-dependent work function of graphene on Pd(111), Appl. Phys. Lett. 97 (2010) 143114.
[16] D. Eom, D. Prezzi, K.T. Rim, H. Zhou, et al., Structure and electronic properties of graphene nano-islands on Co(0001), Nano Lett. 9 (2009) 2844–2848.
[17] Y. Murata, V. Petrova, B.B. Kappes, et al., Moiré superstructures of graphene on faceted nickel islands, ACS Nano 11 (2010) 6509–6514.
[18] M. Yankowitz, et al., Emergence of superlattice Dirac points in graphene on hexagonal boron nitride, Nat. Phys. 8 (2012) 382–386.
[19] T. Ohta, et al., Evidence for interlayer coupling and moiré periodic potentials in twisted bilayer graphene, Phys. Rev. Lett. 109 (2012) 186807.
[20] L.A. Ponomarenko, et al., Cloning of Dirac fermions in graphene superlattices, Nature 497 (2013) 594–597.
[21] I. Pletikosic, et al., Dirac cones and minigaps for graphene on Ir(111), Phys. Rev. Lett. 102 (2009), 056808.
[22] C.R. Dean, et al., Hofstadter's butterfly and the fractal quantum Hall effect in moiré superlattices, Nature 497 (2013) 598–602.
[23] C.M. Seah, S.P. Chai, A.R. Mohamed, Mechanisms of graphene growth by chemical vapor deposition on transition metals, Carbon 70 (2014) 1–21.

[24] T.A. Land, T. Michely, R.J. Behm, J.C. Hemminger, G. Comsa, STM investigation of single-layer graphite structures produced on Pt(111) by hydrocarbon decomposition, Surf. Sci. 264 (1992) 261–270.
[25] J.I. Martínez, P. Merino, A.L. Pinardi, et al., Role of the pinning points in epitaxial graphene moiré superstructures on the Pt(111) surface, Sci. Rep. 6 (2016) 20354.
[26] B. Wang, M. Caffio, C. Bromley, H. Fruchtl, R. Schaub, Coupling epitaxy, chemical bonding, and work function at the local scale in transition metal-supported graphene, ACS Nano 10 (2010) 5773–5782.
[27] C. Busse, et al., Graphene on Ir(111): physisorption with chemical modulation, Phys. Rev. Lett. 107 (2011), 036101.
[28] P. Merino, M. Svec, A.L. Pinardi, et al., Strain-driven moiré superstructures of epitaxial graphene on transition metal surfaces, ACS Nano 5 (2011) 5627–5634.
[29] K. Hermann, Periodic overlayers and moiré patterns: theoretical studies of geometric properties, J. Phys. Condens. Matter 24 (2012) 314210.
[30] A. Artaud, L. Magaud, T.L. Quang, et al., Universal classification of twisted, strained and sheared graphene moiré superlattices, Sci. Rep. 6 (2016) 25670.
[31] R. He, L. Zhao, N. Petrone, et al., Large physisorption strain in chemical vapor deposition of graphene on copper substrates, Nano Lett. 12 (2012) 2408–2413.
[32] X. Shi, Q. Yin, Y. Wei, A theoretical analysis of the surface dependent binding, peeling and folding of graphene on single-crystal copper, Carbon 50 (2012) 3055–3063.
[33] J.Y. Guo, C.X. Xu, F.Y. Sheng, et al., Simulation on initial growth stages of graphene on Pt (111) surface, J. Appl. Phys. 111 (2012), 044318.
[34] D.H. Seo, H.Y. Kim, J.H. Ryu, H.M. Lee, Molecular dynamics simulation of the diffusion of Au and Pt nanoclusters on carbon nanotubes, J. Phys. Chem. C 113 (2009) 10416–10421.
[35] B.H. Morrow, A. Striolo, Morphology and diffusion mechanism of platinum nanoparticles on carbon nanotube bundles, J. Phys. Chem. C 11 (2007) 17905–17913.
[36] A. Stukowski, Visualization, and analysis of atomistic simulation data with OVITO–the Open Visualization Tool, Model. Simulat. Mater. Sci. Eng. 18 (2010), 015012.
[37] S.M. Foiles, M.I. Baskes, M.S. Daw, Embedded-atom-method functions for the fcc metals Cu, Ag, Au, Ni, Pd, Pt, and their alloys, Phys. Rev. B 33 (1986) 7983–7991.
[38] J. Tersoff, Carbon defects and defect reactions in silicon, Phys. Rev. Lett. 64 (1990) 1757–1760.
[39] X.Y. Li, Y.Z. He, Y. Wang, et al., Dewetting properties of metallic liquid film on nanopillared graphene, Sci. Rep. 4 (2014) 3938.
[40] Y.R. Li, Q.X. He, F. Wang, et al., Dynamic evolution study of metal nanofilms on graphite substrates, Acta Phys. Sin. 65 (2016) 239–245.
[41] S. Deng, V. Berry, Wrinkled, rippled and crumpled graphene: an overview of formation mechanism, electronic properties, and applications, Mater. Today 19 (2016) 197–212.
[42] J. Tersoff, Modeling solid-state chemistry: interatomic potentials for multicomponent systems, Phys. Rev. B 39 (1989) 5566–5568.
[43] J. Tersoff, Chemical order in amorphous silicon carbide, Phys. Rev. B 49 (1994) 16349.
[44] Paul Erhart, Karsten Albe, Analytical potential for atomistic simulations of silicon, carbon, and silicon carbide, Phys. Rev. B 71 (2005), 035211.
[45] S. Plimpton, Fast parallel algorithms for short-range molecular dynamics, Comput. Phys. 117 (1995) 1–9.
[46] P. Sule, M. Szendro, C. Hwang, L. Tapaszt, Rotation misorientated graphene moire superlattices on Cu(111): classical molecular dynamics simulations and scanning tunneling microscopy studies, Carbon 77 (2014) 1082–1089.
[47] M. Fuentescabrera, M.I. Baskes, A.V. Melechko, M.L. Simpson, Bridge structure for the graphene/Ni(111) system: a first-principles study, Phys. Rev. B 77 (2008), 035405.
[48] G. Otero, C. Gonzalez, A.L. Pinardi, et al., Ordered vacancy network induced by the growth of epitaxial graphene on Pt(111), Phys. Rev. Lett. 105 (2010) 216102.